Energy sources of field-aligned currents: Auroral electron energization

Andrew N. Wright

Mathematical Institute, University of St. Andrews, St. Andrews, Fife, UK

Received 3 June 2004; revised 27 October 2004; accepted 5 November 2004; published XX Month 2005.

[1] The electron acceleration region in field-aligned currents is considered not as an isolated system but as being embedded in a global circuit. Such a view permits clear identification of the "generator region" and the energy source driving the currents. The global perspective permits a critical appraisal of the appropriateness of using an electric potential to describe the electron acceleration and of criticisms of steady potential acceleration models. We find that ion energy is the source of electron acceleration and that in practice, an electric potential can be useful and appropriate for some circuits.

Citation: Wright, A. N. (2005), Energy sources of field-aligned currents: Auroral electron energization, *J. Geophys. Res.*, *110*, XXXXXX, doi:10.1029/2004JA010609.

1. Introduction

[2] The details of electron acceleration in auroral currents is still a matter of debate. Whether the acceleration is achieved by quasi-steady fields or as inherently time-dependent is still unclear, although the fact that magnetospheric electrons do acquire an energy of several keV above the ionosphere is evident in observations [e.g., *Ergun et al.*, 1998].

[3] Fundamental physics dictates that electron energization must be mediated through the electric field. There is no consensus as to whether this process can be considered as steady (perhaps involving double layers) and an electric potential (as has been used to good effect by *Ergun et al.* [2002a]) or whether equally fundamental physics means no steady energization can be achieved by such a state [*Bryant et al.*, 1992; *Bryant*, 1999, 2002]. That both analyses have some merits is recognized by recent attempts to integrate both aspects in a unified model involving time-dependent stochastic acceleration in addition to a potential electric field. *Janhunen and Olsson* [2000] use stochastic acceleration to drive electrons up the potential hill, whereas *Bryant* [2002] suggests the stochastic acceleration site is at higher altitudes and lies above an isolated potential well. These studies, like most which are motivated by in situ observations, often focus on a segment of the auroral flux tubes and impose a current or voltage generator at the boundaries of the section considered. This does not facilitate a critical appraisal of the issues.

[4] A more suitable framework for an assessment of such questions as (1) why do electrons need to be accelerated, (2) what is the source of the energy that is transferred to the electrons, and (3) is the acceleration process steady is to adopt a global picture of the system in which the acceleration region is embedded. Thus we circumvent the necessity to prescribe an external generator and start from a point of view where clear answers to the above questions may be found.

[5] In this paper the emphasis is on returning to the governing equations and looking at their basic properties. In that sense we do not say anything fundamentally new in this article. The novel aspect comes from interpreting these properties for three simple models (which approximate ULF Alfvén currents, Region 1 currents, and Region 2 currents) and developing some physical understanding of how energy is transferred to the electrons and where the energy is drawn from.

[6] It should be noted that our analysis employs the two-fluid approximation. Thus it will provide the most insight for situations where there is a bulk shift of the entire electron population. In those situations where wave-particle interactions produce detailed features in the distribution function it would be desirable to use a more refined description of the electron dynamics, however, this would make the global nature of our modeling impractical. *Mozer and Hull* [2001] identify three processes that may generate $E_{\|}$ on auroral field lines, namely, high-altitude electron acceleration, a low-altitude sheath, and midaltitude quasi-neutrality maintenance. The approximations we use here are most suitable for studying the midaltitude and high-altitude processes.

2. Spatial and Temporal Scales

[7] A lot of potential confusion comes from misconceptions over what the appropriate spatial and temporal scales are. For example, it is possible to have a local region in which $\partial/\partial t = 0$ (and so $\mathbf{E} = -\boldsymbol{\nabla}\phi$), but outside this region, $\partial/\partial t \neq 0$ and the use of an electric potential is not appropriate. Is such a field steady? The answer must be qualified. It takes a keV energy electron about 1 s to traverse the acceleration region. If the fields vary on a timescale of tens of minutes, although they are not steady, they do not change much on the electron transit time and a "potential" may be very useful. It is analogous to considering someone

0148-0227/05/2004JA010609$09.00

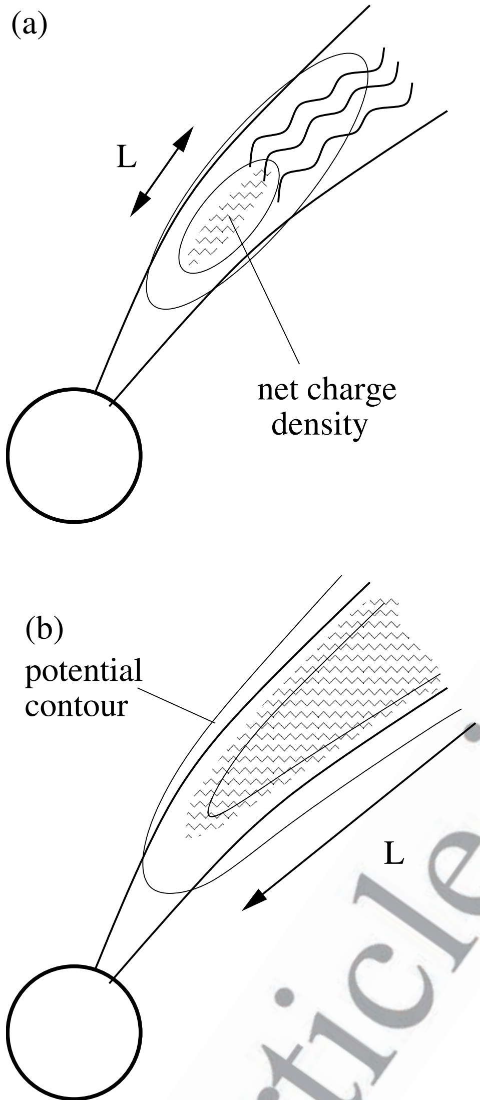

Figure 1. The auroral acceleration region. The hatched region denotes nonzero charge density. (a) The charge is localized and energization may require wave-particle interations. (b) The charge extends over the length of the field line.

skiing down the Himalayas while ignoring the tectonic change in height on the run down.

[8] Although the plasma is quasi-neutral, there is a small but nonzero net charge density (ρ_c) that is associated with the electric field via Poisson's equation, $\nabla \cdot \mathbf{E} = \rho_c/\varepsilon_0$. In Figure 1a, ρ_c is confined within a spatial scale of L, and so the far field solution for the potential must decrease at least as rapidly as $\phi \sim L/r$ (r being the distance from the charge density region). The criticism advanced in the works of *Bryant* [1999] and *Bryant* [2002] is that an electron passing through such a potential can gain no net energy if it starts and finishes sufficiently far away from the center of the potential pattern. Although the electron may gain energy leaving this region, it will have had to expend an equal amount of energy to climb the potential hill to begin with. This is true, but we need to be careful when defining the scale length (L) of ρ_c.

[9] The need for caution regarding L is evident when considering a one-dimensional (1-D) double layer [e.g., *Stern*, 1981, and references therein]. For variations only with the z-coordinate, such a double layer has an extent (Δz) that is typically 20 Debye lengths [*Borovsky*, 1993], and the scale length of ρ_c in a 1-D mathematical model is $L \approx \Delta z$. However, consideration of the physical system this represents, having $\partial/\partial x = \partial/\partial y = 0$, means the charge density extends off to infinity in the (x, y) plane. Thus the physical system has a charge distribution with a scale length $L \to \infty$, and in such a system the electron can never approach from sufficiently far away (several L) for Bryant's criticism to be applied. If the electron is a finite distance from such an idealized double layer, it is effectively starting at the top of the potential hill and so can be energized.

[10] The structure of the double layer is often thought to produce U-shaped contours when sketched in 2-D as shown in Figure 1b [e.g., *Borovsky*, 1993]. The contours may extend along the entire field line until the "generator region" is approached. It is clear that the electrons to be accelerated are enveloped within the potential structure and are certainly not several L away, since L corresponds to the length of the field line and not the thickness of the layer. For such contours it is visibly evident that the electrons are starting at the top of the potential hill and so may be energized. Although this semiglobal contour sketch gives considerable insight, it does not include the generator region, and so questions of how the electrons are supplied at the top of the hill cannot be addressed. Below, we give some global examples which do not suffer from this problem. For the moment, however, we shall consider the three timescales that are crucial in deciding whether it is appropriate to call a potential state like that in Figure 1b "steady."

[11] Here, τ_e is the electron transit time across the double layer, τ_n is the depletion time of electrons from the (finite) reservoir at the top of the hill, and τ_E is the timescale that the electric fields grow and decay over. If $\tau_e \ll \tau_E$, the electric fields are quasi-steady during an electron transit and the use of a potential is helpful. The removal and acceleration of electrons from the reservoir will deplete it, but if $\tau_E \ll \tau_n$, the depletion is not significant and may be treated as steady [*Wright et al.*, 2002].

[12] There is mounting observational evidence of upward moving ions [*Ergun et al.*, 2002a] and electrons [*Carlson et al.*, 1998] whose energy is consistent with the potential calculated from $\int \mathbf{E} \cdot ds$ along the spacecraft trajectory. The importance of this has been recognized in the model of *Janhunen and Olsson* [2000], who use closed potential contours (which can provide no net steady energization) and wave particle interactions at higher altitudes to energize the electrons so they may climb the potential hill.

3. Global Models

[13] Global models of magnetospheric currents often employ the single-fluid MHD (magnetohydrodynamic) approximation and have the great advantage that the global picture includes the generator region. However, they have the disadvantage that the electron mass is neglected in this approximation, meaning the electrons have vanishing kinetic energy and rendering a discussion of electron

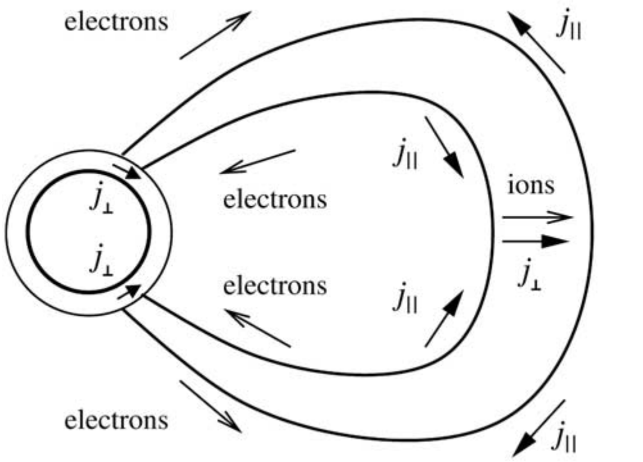

Figure 2. A snapshot of the current system for the fundamental standing Alfvén mode and the particles responsible for carrying the currents. Half a cycle later, the currents and velocities will have switched sign.

energization meaningless. *Wright et al.* [2002] showed how two-fluid MHD (employing an electron fluid and a separate ion fluid) retains a finite electron mass and can be viewed as a correction to the leading-order single-fluid MHD solution and allows us to consider electron energetics. This is the approach we adopt here.

3.1. Generation of $j_\parallel$

[14] We begin with a consideration of how field-aligned currents arise from the single-fluid MHD momentum equation

$$\rho \frac{d\mathbf{v}}{dt} = \mathbf{j} \times \mathbf{B} - \boldsymbol{\nabla} p + \mathbf{F}. \tag{1}$$

The symbols have their usual meanings. When considering a localized region, **F** could represent some driving force on the boundary associated with the generator region. In a global model we do not need **F**. Equation (1) may be used to define $\mathbf{j}_\perp$

$$\mathbf{j}_\perp = -\left(\rho \frac{d\mathbf{v}}{dt} + \boldsymbol{\nabla} p - \mathbf{F}\right) \times \mathbf{B}/B^2. \tag{2}$$

Wright et al. [2002] stress that the net charge density (ρ_c) evolves according to $\partial\rho_c/\partial t + \boldsymbol{\nabla} \cdot \mathbf{j} = 0$. To understand how $j_\parallel$ is generated, consider a situation in which $j_\parallel$ is initially zero. Equation (2) gives $\mathbf{j}_\perp$, and in general $\boldsymbol{\nabla} \cdot \mathbf{j}_\perp \neq 0$, so there will be a build up of net charge density initially. From $\boldsymbol{\nabla} \cdot \mathbf{E} = \rho_c/\varepsilon_0$, we find that the electric field associated with ρ_c will have a component parallel to **B** which causes electrons to flow ($v_{e\parallel} \neq 0$) and carry a field-aligned current ($j_\parallel \neq 0$) such that $\boldsymbol{\nabla} \cdot \mathbf{j} \approx 0$ and the build up of ρ_c is reduced to small (quasi-neutral) values.

3.2. Generation of $E_\parallel$

[15] Although a global single-fluid MHD description can identify the source of $j_\parallel$ generation and location of electron acceleration, we need to adopt a two-fluid model (i.e., finite m_e) to describe electron energization.

[16] For simplicity we consider a cold electron fluid governed by

$$m_e\left(\frac{\partial \mathbf{v}_e}{\partial t} + (\mathbf{v}_e \cdot \boldsymbol{\nabla})\mathbf{v}_e\right) = -e(\mathbf{E} + \mathbf{v}_e \times \mathbf{B}). \tag{3}$$

The parallel component of (3) in the auroral acceleration region is [*Wright et al.*, 2002]

$$E_\parallel \approx -\frac{m_e}{e}\left(\frac{\partial v_{e\parallel}}{\partial t} + \left(v_{e\parallel}\nabla_\parallel\right)v_{e\parallel}\right), \tag{4}$$

and for typical ULF parameters $(v_{e\parallel}\nabla_\parallel)v_{e\parallel} \gg \partial v_{e\parallel}/\partial t$, indicating the importance of treating electron dynamics nonlinearly [*Rönnmark*, 1999].

3.3. Energy Considerations

[17] The retention of finite m_e in the two-fluid approximation allows an examination of electron energization within a global view and identification of the energy source. Taking the scalar product of $\mathbf{v}_e$ and equation (3) gives, after some manipulation,

$$\frac{\partial}{\partial t}\left(\frac{1}{2} n m_e v_e^2\right) + \boldsymbol{\nabla} \cdot \left(\frac{1}{2} n m_e v_e^2 \mathbf{v}_e\right) = -ne\mathbf{v}_e \cdot \mathbf{E}. \tag{5}$$

[18] A similar equation may be derived for the ion fluid, except that we allow for it to be a warm adiabatic fluid of pressure p_i, as ion pressure can be significant in some situations;

$$\frac{\partial}{\partial t}\left(\frac{1}{2} n m_i v_i^2 + \frac{p_i}{\gamma - 1}\right) + \boldsymbol{\nabla} \cdot \left(\frac{1}{2} n m_i v_i^2 \mathbf{v}_i + \frac{\gamma p_i}{\gamma - 1}\mathbf{v}_i\right) = ne\mathbf{v}_i \cdot \mathbf{E}. \tag{6}$$

The final energy equation we need follows from the scalar product of **B** with the induction equation

$$\frac{\partial}{\partial t}\left(\frac{B^2}{2\mu_0}\right) + \boldsymbol{\nabla} \cdot (\mathbf{E} \times \mathbf{B}/\mu_0) = -\mathbf{j} \cdot \mathbf{E}. \tag{7}$$

The left-hand sides of equations (5), (6), and (7) represent continuity of electron, ion, and magnetic energies, respectively. The right-hand sides represent sources of these different energy densities. Noting that $\mathbf{j} = ne(\mathbf{v}_i - \mathbf{v}_e)$, we see the sum of (5), (6), and (7) has a right-hand side that vanishes, while the left-hand side expresses conservation of total energy. From each of the individual energy equations (5), (6), and (7) it is evident that the electric field is responsible for the exchange of energy between electrons, ions, and magnetic field. In the following global current systems we shall use this approach to see how electrons are energized at the expense of ion and magnetic energies.

4. ULF Alfvén Wave

[19] Figure 2 shows a snapshot of a meridional slice of an axisymmetric fundamental standing Alfvén wave. The single-fluid model has worked well for calculating the gross features of these waves. With the present interest in electron acceleration, *Wright et al.* [2002] have added

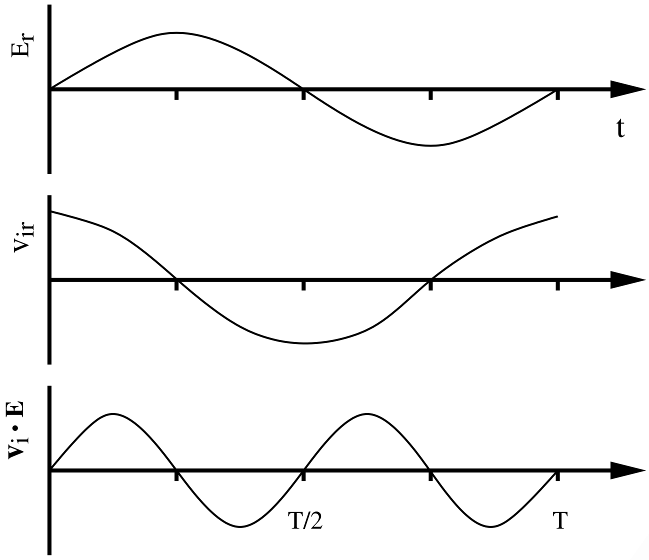

Figure 3. The variation of E_r, the ion polarization drift v_{ir}, and the ion energy source term $ne\mathbf{v}_i \cdot \mathbf{E}$ over one cycle in the equatorial plane.

finite m_e corrections to the single-fluid model. Their analysis showed how (for a cold ion fluid, $p_i = 0$) the inertial ($\rho d\mathbf{v}/dt$) term in (2) is associated with the polarization current. It maximizes in the equatorial region and is carried by ions, whose perpendicular velocity is

$$\mathbf{v}_{\perp i} = \frac{\mathbf{E}\times\mathbf{B}}{B^2} + \frac{\mathbf{j}_\perp}{ne}. \qquad (8)$$

The latter term (the polarization drift) is smaller than the $\mathbf{E}\times\mathbf{B}$ drift by $\omega/\omega_{ci} \sim 10^{-3}$ for typical parameters, so the ions essentially $\mathbf{E}\times\mathbf{B}$ drift in the azimuthal direction. The smaller polarization drift of the ions at the equator is indicated in Figure 2 and begins to produce a net charge density. The $E_\|$ associated with this charge accelerates electrons along $\mathbf{B}$ to maintain quasi-neutrality. So where does the energy to accelerate the electrons come from? We begin by considering the solution in the equatorial plane, where on a given L shell, $\mathbf{E} = E_r\hat{\mathbf{r}}$ and we may choose $E_r = E_0 \sin(\omega_A t)$, ω_A being the Alfvén wave frequency. From (8) the leading ion drift is $\mathbf{E}\times\mathbf{B}/B^2 = (E_r/B_0)\hat{\phi}$, i.e., $v_{i\phi} = (E_0/B_0)\sin(\omega_A t)$ in the equatorial plane. This is identical, to leading order, to the single fluid v_ϕ and may be used with (2) to find the polarization current and hence the polarization drift (8)

$$v_{ir} = \frac{-\rho}{neB^2}\frac{d}{dt}\left(\frac{\mathbf{E}\times\mathbf{B}}{B^2}\right)\times\mathbf{B}\cdot\hat{\mathbf{r}} \approx \frac{\omega_A}{\omega_{ci}}\cdot\frac{E_0}{B_0}\cos(\omega_A t). \qquad (9)$$

[20] Figure 3 shows the variation of E_r and v_{ir} over one wave cycle, and the bottom part displays $\mathbf{v}_i \cdot \mathbf{E}$ which represents the addition or removal of energy from the ions. (See the right-hand side of equation (6).) Evidently, from the v_{ir} and $v_{i\phi}$ components, the ion fluid elements follow elliptical orbits in the equatorial plane (see Figure 4). During the first quarter of a cycle ($0 < t < T/4$), E_r and v_{ir} are positive so the ions gain energy, reaching their maximum speed at $t = T/4$. During $T/4 < t < T/2$, v_{ir} is negative so energy is extracted from the ions and their kinetic energy is minimized at $t = T/2$. For the second half of the cycle, E_r is negative, so the ions' kinetic energy increases until $t = 3T/4$, at which time v_{ir} switches sign and the ions lose energy by slowing down until $t = T$.

[21] If m_e is neglected, (5) indicates that $\mathbf{v}_e \cdot \mathbf{E} = 0$, so energy is just exchanged between the ion kinetic energy (centered on the equatorial section) and magnetic energy (concentrated toward the ionosphere) [e.g., *Wright et al.*, 2003]. This is the situation described by single-fluid MHD in which the work done on the ion fluid ($ne\mathbf{v}_i \cdot \mathbf{E}$) may be reexpressed as the work done on a neutral single-fluid ($\mathbf{v}\cdot\mathbf{j}\times\mathbf{B}$). The equivalence follows from the single-fluid Ohm's Law $\mathbf{E} + \mathbf{v}\times\mathbf{B} = 0$ and (8), and the two descriptions are just different interpretations in the single- and two-fluid MHD models.

[22] In an Alfvén normal mode with $m_e = 0$ there is no electron energization ($\mathbf{v}_e \cdot \mathbf{E} = 0$) and energy is simply exchanged between ion kinetic and magnetic energies with the Poynting vector transporting energy along the field line. There is no causality in such an energy cycle and neither energy is more fundamental than the other, although we can say that according to (2) the ion inertia leads to the generation of the field-aligned current. When m_e is finite there is a relatively small electron energy density, so we would not regard the electrons as driving the mode. Rather, the ion and magnetic energies are the main energy reservoirs, but their exchange (when m_e is finite) requires an $\mathbf{E}$ that energizes the electrons [*Wright et al.*, 2003]. Thus it seems appropriate to say that the electrons are energized at the expense of the ion and magnetic energies. In fact, if we view the system starting at the time when there is no energy in the electrons (i.e., $\mathbf{j} = 0$), then all the energy is in the form of ion kinetic energy. This is subsequently largely given up to the magnetic field energy, with a small fraction going into the electron energy. Thus it is most accurate to say the electrons are energized at the expense of the ion energy. Indeed, *Wright et al.* [2003] have shown that this can represent a significant dissipation mechanism for the ULF Alfvén waves.

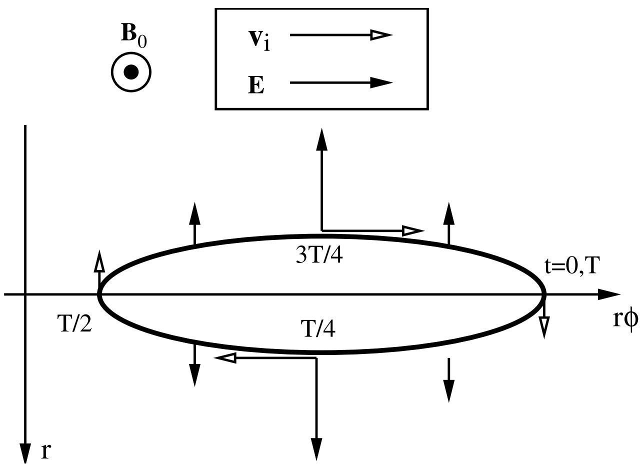

Figure 4. A view in the equatorial plane of an ion fluid element's elliptical trajectory and electric field it experiences over one wave cycle.

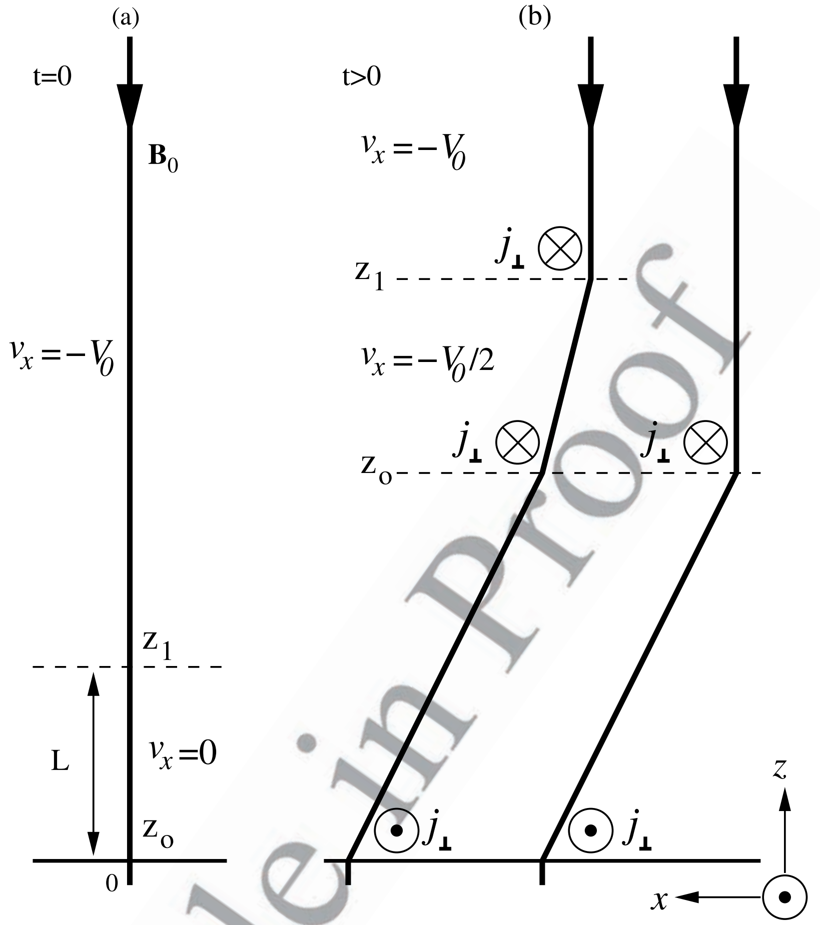

Figure 5. A simple model for the one-dimensional evolution of an open field line from (a) the initial state. At (b) later times, two wave fronts propagate away from the Earth at $z_0 = V_A t$ and $z_1 = V_A t + L$, where perpendicular currents flow. For $0 < z < z_0$ the plasma moves with $v_x = -V_0/(1 + \mu_0 \Sigma_p V_A)$ and an ionospheric Pedersen current flows at $z = 0$. The right-hand field line in Figure 5b is a simplified model for which the wave front currents have been combined in a single location ($z_1 \rightarrow z_0$).

[23] Regarding the question of whether an electric potential is useful for describing electron energization, the electron transit time ($\sim$1 s) is much less than the wave period ($\sim$100 s) so the fields are effectively stationary. Also, the large volume of the flux tube means the electron content is not depleted significantly over a cycle [*Wright et al.*, 2002]. The electrons are effectively described as being released from a large reservoir at the top of a potential hill.

5. Region 1 Currents

[24] The differing behavior of field lines across the open/closed field line boundary gives rises to magnetic shear associated with part of the region 1 current system. In this section we shall consider the acceleration of electrons in these currents, and the applicability of the notions of "steady state" and the use of an electric potential.

[25] A simple one-dimensional model for the evolution of recently opened field lines was given by *Wright* [1996] and is summarized in Figure 5. At $t = 0$ the field line is straight ($-B_0\hat{\mathbf{z}}$) and has a magnetosheath section ($z > L$) moving with the sheath flow speed ($-V_0\hat{\mathbf{x}}$), while the magnetospheric section is at rest. At $z = 0$ there is an ionospheric boundary characterized by a height-integral Pedersen conductivity (Σ_p). The density is uniform as is the equilibrium Alfvén speed (V_A). The single-fluid MHD model shows this initial condition launches Alfvén waves which are subsequently located at $z_0 = V_A t$ and $z_1 = V_A t + L$. The speeds of the different sections are shown in Figure 5b.

[26] Note the perpendicular currents that are responsible for slowing the sheath flow as they propagate out and for heating the ionosphere. In the single-fluid description the kinetic energy of the sheath flow is stored as magnetic energy (in the tilted field section) and dissipated through ionospheric heating. In the previous section there was no causality implicit in the single fluid normal mode. This is not true of the Alfvén wave in Figure 5, where it is evident that the energy is initially in the form of kinetic energy and converted to magnetic energy and ionospheric heating.

[27] The two kinks in the left-hand magnetic field line in Figure 5b are a result of our initial condition, and other models of magnetosphere-ionosphere coupling have combined these into a single kink [e.g., *Southwood and Hughes*, 1983]. This limit may be obtained by letting $L \rightarrow 0$, so $z_1 \rightarrow z_0$. The result is shown as the right-hand field line in Figure 5b and for simplicity will be adopted from now on.

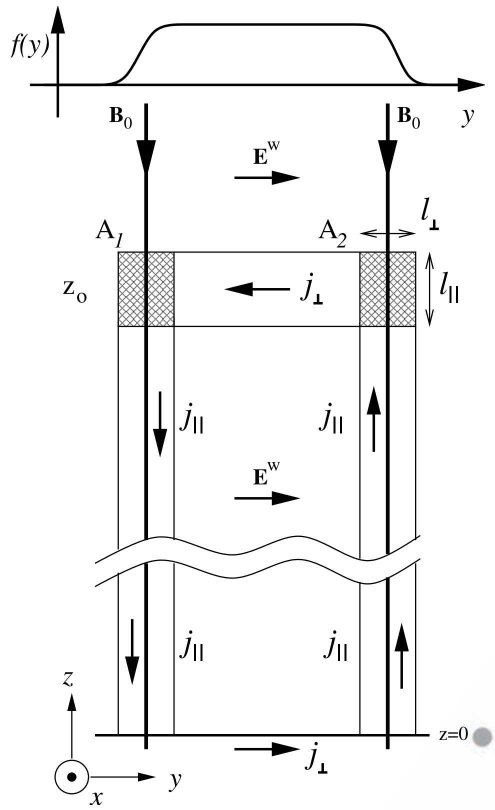

Figure 6. A two-dimensional model of the current circuit in Figure 5. The perpendicular current at z_0 is diverted into field-aligned current at the hatched regions A_1 and A_2, where electrons are accelerated to meet current continuity. The top section may be viewed from a frame moving with the wavefront in which the fields are (locally) stationary.

[28] In Figure 6 a two-dimension model of the current circuit associated with the right-hand field line of Figure 5b is illustrated. The perpendicular current at z_0 is diverted into field-aligned current at the hatched regions A_1 and A_2 where electrons are accelerated to meet current continuity. The top section may be viewed from a frame moving with the wavefront in which the fields are (locally) stationary. The electric field in this frame ($\mathbf{E}^w$) will be different from that in the Earth's frame.

[29] Figure 5 represents a one-dimensional system and so only has $\mathbf{j}_\perp$. To investigate the full current circuit, we need to account for the fact that the polar cap has a finite width and may be allowed for by simply letting Σ_p be localized in y according to the envelope $f(y)$ shown in Figure 6. The current now flows in a circuit with field-aligned (Birkeland) currents connecting the ionosphere and outward propagating wavefront. Behind the wavefront the solution is steady, so a potential is useful here. Indeed, if a realistic converging field geometry was employed above the ionosphere, electron acceleration would be required here (as in the previous section); however, unlike that example, the present system is locally exactly steady. Of course the whole system (including the wavefront) in Figure 6 is not steady, and it is the propagation of the wavefront along an infinite open flux tube that allows access to an infinite reservoir of electrons to feed the upward current. The downward current must be fed by accelerating ionospheric electrons upward, which may in principle ultimately deplete the ionosphere unless there is sufficient photoionization of neutrals.

[30] *Damiano and Wright* [2005] have studied electron acceleration in a propagating Alfvén current loop whose front half resembles the wavefront in Figure 6. Allowing the currents to be distributed over a width $\ell_\perp$ (in y) and $\ell_\parallel$ (in z), they show how there is an $E_\parallel$ at the region marked A_1 and A_2 where the electrons are accelerated to carry the required $j_\parallel$. This type of calculation, and the discussion below, provides much insight into the ideas first advanced by *Goertz and Boswell* [1979], who first suggested that electron inertia could be important in Alfvénic models of ionosphere-magnetosphere coupling.

5.1. Field Lines With $j_\parallel = 0$

[31] A detailed analysis of the energy balance around $z = z_0$ is facilitated by considering field lines on which $j_\parallel = 0$ (i.e., they do not intersect A_1 or A_2). In the plasma frame the ion energy density source term (right-hand side of (6)) is $ne\mathbf{v}_i \cdot \mathbf{E} = nev_{iy}E_y < 0$ (v_{iy} is the polarization drift of the ions $\approx j_y/ne < 0$ and $E_y = v_xB_z \geq 0$). The electron source term is $-ne\mathbf{v}_e \cdot \mathbf{E} = -nev_{ey}E_y < 0$. (The v_{ey} is the much smaller polarization drift of the electrons $v_{ey} \approx -(m_e/m_i)v_{iy}$ and is positive.) The magnetic energy source term $-\mathbf{j} \cdot \mathbf{E} = -j_yE_y \equiv -ne(v_{iy} - v_{ey})E_y > 0$. Thus both electrons and ions lose kinetic energy, while the magnetic energy increases.

[32] Transforming to the frame of reference of the wavefront gives a single-fluid solution for which $\partial/\partial t = 0$ locally. The electric field in the wavefront frame is $\mathbf{E}^w = -\mathbf{v} \times \mathbf{B}_0 - \mathbf{V}_A \times \mathbf{b} = V_0B_0\hat{\mathbf{y}}$, where we have used the relation for an Alfvén wave propagating antiparallel to B_0 for illustrative purposes:

$$\Delta v_x = -\frac{\Delta b_x}{\sqrt{\mu_0\rho}} \tag{10}$$

and $v_x = -V_0 + \Delta v_x$ represents the x component of the plasma velocity in the Earth's rest frame. Since $E_y^w > 0$ and the polarization drifts v_{iy} and v_{ey} are unchanged by the transformation, we find a similar interpretation to that of the plasma frame. The magnetic field energy increases at the expense of the electron and ion energies.

5.2. Field Lines With $j_\parallel \neq 0$

[33] Field lines for which $j_\parallel \neq 0$ will have additional energy considerations as electrons and ions have a nonzero field-aligned acceleration. Remaining in the wavefront frame for the moment, the electron and ion velocities are

$$\mathbf{v}_e^w = -V_A\hat{\mathbf{z}} + \mathbf{v}_e, \qquad \mathbf{v}_i^w = -V_A\hat{\mathbf{z}} + \mathbf{v}_i. \tag{11}$$

In the single-fluid ($m_e/m_i \to 0$) limit $\mathbf{E}^w = V_0B_0\hat{\mathbf{y}}$, and for finite m_e there will be a small correction. The leading-order $\mathbf{E}_\perp^w$ is unchanged, but $E_\parallel \equiv E_\parallel^w$ now becomes nonzero. Note from (11) that v_{ey}^w and v_{iy}^w are the same as in the previous section. However, field lines passing through A_2 have electrons approaching from $z = \infty$ with $v_{e\parallel}^w = V_A$ and being speeded up on exiting A_2. Similarly, ions approach with $v_{i\parallel}^w = V_A$ and are slowed down slightly on leaving.

[34] For simplicity we shall assume that the change in electron speed is small compared with the Alfvén speed,

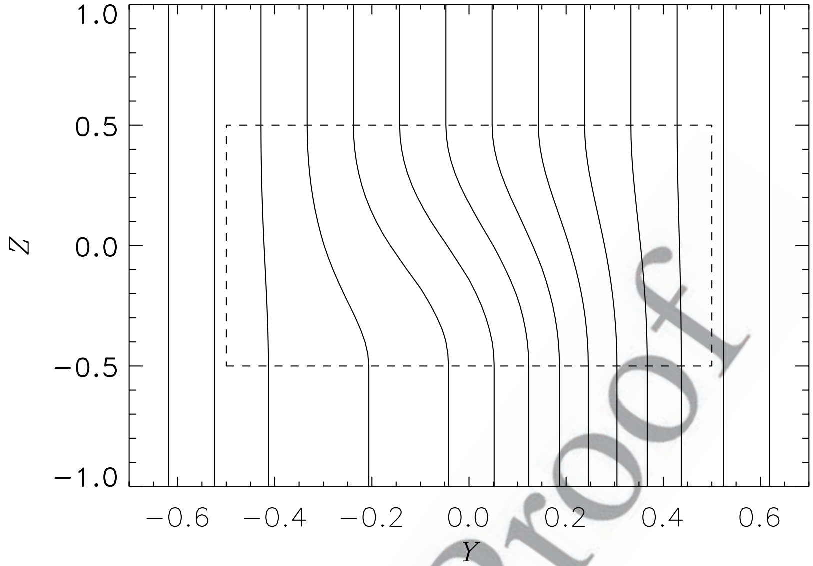

Figure 7. The variation of potential in the wavefront frame with $Y = y/\ell_\perp$ and $Z = (z - z_0)/\ell_\parallel$ centered on the acceleration region A_2 of Figure 6. Electrons move along magnetic field lines (Y = constant) and so cross potential contours and change their energy.

which is likely to be the case for the magnetosphere. This assumption places a constraint upon the amplitude of the Alfvén wave (taken as V_0). Noting that $|v_{e\parallel}| = j_\parallel/ne$, $|j_\parallel| = b_x/\mu_0\ell_\perp$, $|b_x| = V_0B_0/V_A$, gives

$$\frac{v_{e\parallel}}{V_A} = \frac{V_0}{V_A}\cdot\sqrt{\frac{m_i}{m_e}}\cdot\frac{\lambda_e}{\ell_\perp} \ll 1, \tag{12}$$

where λ_e is the electron inertial length ($\lambda_e^2 = m_e/\mu_0 ne^2$).

[35] Taking the solution to be steady in the neighborhood of z_0, we can write $\mathbf{E}^w = -\boldsymbol{\nabla}\phi$. The leading behavior of $\mathbf{E}_\perp^w$ is described by a potential $-V_0B_0y$, while there is an additional (smaller) contribution associated with $E_\parallel$. The latter can be derived from energy conservation of an electron fluid element moving along a field line (i.e., y = constant) from $z = +\infty$ where its total energy density is W

$$W = \frac{1}{2}nm_e\left(V_A + v_{e\parallel}(y,z)\right)^2 - ne\phi(y,z) \equiv \frac{1}{2}nm_eV_A^2. \tag{13}$$

For $v_{e\parallel}/V_A \ll 1$ and noting $j_\parallel = -nev_{e\parallel}$, (13) gives the total potential as

$$\phi = -V_0B_0y + \frac{m_e}{e}V_Av_{e\parallel} = -V_0B_0y - \frac{m_e}{ne^2}V_Aj_\parallel, \tag{14}$$

which contains the leading-order term associated with the background flow and a correction for finite m_e.

[36] Figure 7 shows potential contours. For clarity we chose $(\lambda_e/\ell_\perp)^2 = 0.2$, although it is likely to be much smaller than this in practice. The dashed region outlines the acceleration region A_2, and the form of the contours is similar to that of the weak double layer shown in Figure 3d of *Eriksson and Boström* [1993]. As electrons traverse the box in Figure 7, they do so along a field line (y = constant) and so slip down a potential slope, thus being accelerated. In contrast, ions are decelerated. The potential in (14) reduces to that employed by *Damiano and Wright* [2005] in the limit $V_0 = 0$. They showed excellent agreement between the $E_\parallel$ predicted by (14) with that from their simulation.

[37] The consideration of the energy sources in equations (5), (6), and (7) is similar to the previous subsection for terms involving $\mathbf{E}_\perp^w$. We need only study the additional terms involving $E_\parallel^w$ here. (Note $E_\parallel^w \equiv E_\parallel$.) At A_2 there is an additional electron energy source term of $-nev_{e\parallel}^wE_\parallel \approx -neV_AE_\parallel > 0$ (note $E_\parallel = \mathbf{E}\cdot\mathbf{B}_0/B_0 < 0$ and we have assumed $v_{e\parallel}/V_A \ll 1$), so electrons gain energy. The additional ion energy source is $nev_{i\parallel}^wE_\parallel \approx neV_AE_\parallel < 0$, so ions lose energy at precisely the rate electrons gain it based upon field-aligned motion. There is an additional magnetic energy source term much smaller than these of $-j_\parallel E_\parallel$, however $j_\parallel E_\parallel/j_\perp E_\perp^w \approx \lambda_e^2/\ell_\perp^2 \ll 1$, so the leading behavior of the magnetic field energy is unchanged. This relation may be shown by noting $|j_\parallel|/\ell_\parallel \approx |\mathbf{j}_\perp|/\ell_\perp$ and

$$\frac{E_\parallel}{E_\perp^w} \approx \frac{\Delta\phi}{\ell_\parallel}\cdot\frac{1}{V_0B_0} \approx \frac{\lambda_e^2}{\ell_\parallel\ell_\perp}, \tag{15}$$

the latter equality following from (14), $|j_\parallel| \approx b_x/\mu_0\ell_\perp$, and (10) with $\Delta v_x \approx V_0$.

[38] The details of energy balance are frame-dependent, and in the wave frame the region A_2 is where electrons are energized at the expense of ion energy. In contrast, in the region A_1 ions are energized at the expense of electron energy. In this frame the use of a local potential is useful.

[39] We now consider energy balance on $j_\parallel \neq 0$ field lines in the vicinity of the wavefront but in the terrestrial frame of reference (i.e., the wavefront is at $z_1 = V_At$ and propagates away from the Earth). The analysis of $j_\parallel = 0$ field lines shows how the kinetic energy of both electrons and ions is reduced (due to polarization drifts along $\hat{\mathbf{y}}$) after encountering the wavefront, while the magnetic energy behind the wavefront increases. The effect of $E_\parallel \neq 0$ (as on field lines for which $j_\parallel \neq 0$) leads to extra source terms. There is an additional electron energy source of $-nev_{e\parallel}E_\parallel > 0$, and an

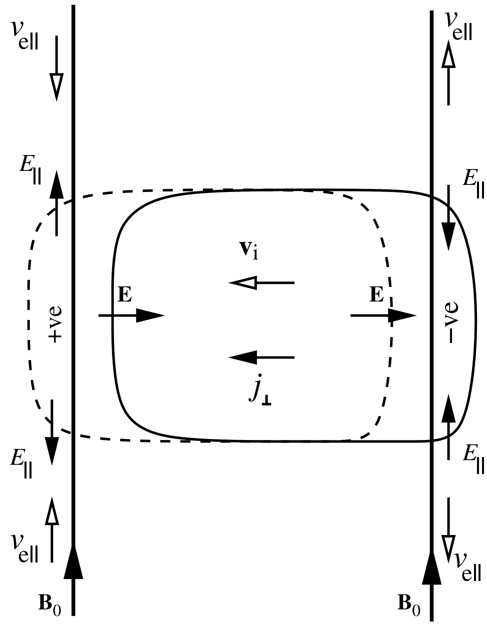

Figure 8. A warm ion cloud centered on the equatorial plane at midnight (solid line), viewed from the magnetotail looking earthward, drifts westward (dashed line) carrying a current and setting up a charge separation that causes electrons to carry a field-aligned current at the edges.

ion source of $nev_{i\|}E_{\|} > 0$ at both A_1 and A_2 so electrons and ions gain energy; however, the ion source is less than that of the electrons by m_e/m_i. The new contribution to the magnetic energy source is $-j_{\|}E_{\|} < 0$ at both A_1 and A_2, so the magnetic field energy is reduced but only slightly, since $j_{\|}E_{\|}/j_{\perp}E_{\perp} \approx \lambda_e^2/\ell_{\perp}^2 \ll 1$. Hence the basic energy balance is still that of ion kinetic energy ($\frac{1}{2}nm_iv_{i\perp}^2$) being converted to magnetic energy, but a small fraction of the ion kinetic energy goes into electron energization as well.

[40] It is evident that the use of a local potential in the wave frame can provide much insight, and the use of a "steady" model is appropriate locally, although globally the solution is time-dependent. On open field lines there is an infinite supply of electrons for upward currents, so the reservoir will not be depleted. A gravitational analogy of their acceleration would be to consider the motion of ball bearings on a raised horizontal track. The propagation of the Alfvén wave would correspond to moving the section of track behind the wavefront to a lower (but constant) height. At the wavefront the track will be inclined between the two levels, and ball bearings will roll down the slope gaining energy and then roll along the lower section at constant speed before being dumped off the end of the track (ionosphere).

6. Region 2 Currents

[41] The Region 2/ring current circuit is driven by hot plasma from the magnetotail reaching dipolar-like closed field lines. (See the lucid account by *Cowley* [2000, and references therein].) To illustrate the basic process of $j_{\|}$ generation and electron energization, we consider the simplified system shown in Figure 8, which is viewed from the magnetotail looking earthward. The solid line is the boundary of a warm plasma cloud centered on the equatorial plane by particle mirroring. The curvature and gradient drifts move the ions westward and electrons eastward, giving rise to the ring current ($\mathbf{j}_{\perp}$). These drifts are energy-dependent, and in this example we take a hot ion population ($p_i \neq 0$) and neglect the electron pressure.

[42] The structure of the ring current is most easily envisaged in terms of particle rather than fluid behavior. Although we do not present a detailed solution here, we note that gradient and curvature drifts do not change the kinetic energy of an ion (i.e., the internal and kinetic energies in the fluid description). Such a change would arise from an electric field, the origin of which is easiest to see within the particle description also. After some time the ion drifts have moved the hot ion fluid to the location identified by the dashed line in Figure 8. The original neutral configuration begins to develop an excess of positive charge on the western side and negative charge on the eastern side. The electric field associated with this charge imbalance is indicated in the figure. On the western edge, $E_{\|}$ acts to draw electrons into the positively charged region and keep it quasi-neutral. The electron energy source term here is $-nev_{e\|}E_{\|} > 0$, so electrons are energized. On the eastern edge, $E_{\|}$ expels electrons from the negative region to maintain quasi-neutrality. Here $-nev_{e\|}E_{\|} > 0$ again, so electrons gain energy on this side too. The source of electron energization may be seen by considering the central section. The magnetic energy source term $-\mathbf{j} \cdot \mathbf{E} > 0$, so the magnetic field energy increases (associated with $\nabla \times \mathbf{B} = \mu_0\mathbf{j}_{\perp}$). However, the ion energy source term $ne\mathbf{v}_i \cdot \mathbf{E} < 0$, indicating ion energy is lost.

[43] The overall picture is of a warm ion cloud drifting westward while losing energy. The energy given up goes in to energizing the Region 2 field-aligned current-carrying electrons and distorting the magnetic field. A more complete description of this model is beyond the scope of the present article. The cursory discussion above draws on both guiding center and fluid concepts to clarify some of the underlying physical processes that will govern the system.

7. Concluding Remarks

[44] Electron acceleration in Birkeland currents such as those in the Region 1 and 2 currents and standing Alfvén waves has been considered from a global perspective such that the accelerator region and the generator region are both clearly identifiable. A two-fluid model is adopted (being the simplest description that permits an analysis of electron energization) and necessarily restricts the type of processes we are able to consider. However, this is sufficient for identifying energy exchanges and considering issues related to large time and space scales.

[45] In the introduction we enumerated a few key questions to which we now return. (1) Why do electrons need to be accelerated? Within the detailed examples considered in this paper, the electrons move to carry a field-aligned current so that $\nabla \cdot \mathbf{j} \approx 0$ and the plasma can remain quasi-neutral. Several mechanisms can give rise to $\mathbf{j}_{\perp}$ (e.g., ion polarization, gradient, and curvature drifts) which will violate charge neutrality if a suitable $j_{\|}$ (i.e., field-aligned electron motion) is not generated. (2) What is the source of energy that is transferred to the electrons? The details of energy exchange between ions, electrons, and the magnetic

field are frame-dependent. In the terrestrial frame it is a general feature that ion energy is given up and converted to magnetic energy and energized electrons. (3) Is the acceleration process steady? Although a system may not be exactly steady in a mathematical sense, it may be for practical purposes, in the sense that the fields and equilibrium do not change significantly over the acceleration timescale. For such a system an electric potential may be useful, and contours can extend along most of the field line requiring large sections of flux tubes to be slightly charged (although quasi-neutral). Criticisms relating to the inability of localized charge distributions to provide energization are not applicable to such a system as the charge density is not localized over a scale that is small compared with the particle path length.

[46] The latter comments are pertinent to reported observations of double layers in downward [*Andersson et al.*, 2002] and upward [*Ergun et al.*, 2002b; *Hull et al.*, 2003] current regions. Ergun et al. suggest that up to half of the electron energy can be supplied by one double layer. Particularly for upward currents, it is possible that these double layers are associated with steady fields and particle energization (in the sense of section 2, $\tau_e \ll \tau_E \ll \tau_n$). This would require the potential contours to map out along the length of the current carrying flux tubes in a similar fashion to that shown in Figure 1b [see also *Wright et al.*, 2003]. At low altitudes, double layers may be formed by having adjacent contours in close proximity.

[47] **Acknowledgments.** The author would like to thank W. Allan, P. Damiano, T. Neukirch, and K. Rönnmark for helpful discussions and the referees for their constructive comments.

[48] Lou-Chuang Lee thanks Bill Allan and another reviewer for their assistance in evaluating this paper.

References

Andersson, L., R. E. Ergun, D. L. Newman, J. P. McFadden, C. W. Carlson, and Y.-J. Su (2002), Characteristics of parallel electric fields in the downward current region of the aurora, *Phys. Plasmas*, *9*(8), 3600, doi:10.1063/1.1490134.

Borovsky, J. E. (1993), The strong-double-layer model of auroral arcs: An assessment, in *Auroral Plasma Dynamics*, *Geophys. Monogr. Ser.*, vol. 80, edited by R. L. Lysak, p. 113, AGU, Washington, D. C.

Bryant, D. A. (1999), Electron acceleration in the aurora and beyond, Inst. of Phys., Philadelphia, Penn.

Bryant, D. A. (2002), The roles of static and dynamic electric fields in the auroral acceleration region, *J. Geophys. Res.*, *107*(A3), 1077, doi:10.1029/2001JA900162.

Bryant, D. A., R. Bingham, and U. de Angelo (1992), Double layers are not particle accelerators, *Phys. Rev. Lett.*, *68*, 37.

Carlson, C. W., et al. (1998), FAST observations in the downward auroral current region: Energetic upgoing electron beams, parallel potential drops, and ion heating, *Geophys. Res. Lett.*, *25*, 2017.

Cowley, S. W. H. (2000), Magnetosphere-ionosphere interactions: A tutorial review, in *Magnetospheric Current Systems*, *Geophys. Monogr. Ser.*, vol. 118, edited by S.-I. Ohtani et al., p. 91, AGU, Washington, D. C.

Damiano, P. A., and A. N. Wright (2005), Two-dimensional hybrid MHD-kinetic electron simulations of an Alfvén wave pulse, *J. Geophys. Res.*, *110*, A01201, doi:10.1029/2004JA010603.

Ergun, R. E., et al. (1998), FAST satellite observations of electric field structures in the auroral zone, *Geophys. Res. Lett.*, *25*, 2025.

Ergun, R. E., et al. (2002a), Parallel electric fields in the upward current region of the aurora: Indirect and direct observations, *Phys. Plasmas*, *9*, 3685.

Ergun, R. E., L. Andersson, D. Main, Y.-J. Su, D. L. Newman, M. V. Goldman, C. W. Carlson, J. P. McFadden, and F. S. Mozer (2002b), Parallel electric fields in the upward current region of the aurora: Numerical solutions, *Phys. Plasmas*, *9*(9), 3695, doi:10.1063/1.1499121.

Eriksson, A. I., and R. Boström (1993), Are weak double layers important for auroral particle acceleration?, in *Auroral Plasma Dynamics*, *Geophys. Monogr. Ser.*, vol. 80, edited by R. L. Lysak, p. 105, AGU, Washington, D. C.

Goertz, C. K., and R. W. Boswell (1979), Magnetosphere-ionosphere coupling, *J. Geophys. Res.*, *84*, 7239.

Hull, A. J., J. W. Bonnell, F. S. Mozer, J. D. Scudder, and C. C. Chaston (2003), Large parallel electric fields in the upward current region of the aurora: Evidence for ambipolar effects, *J. Geophys. Res.*, *108*(A6), 1265, doi:10.1029/2002JA009682.

Janhunen, P., and A. Olsson (2000), New model for auroral acceleration: O-shaped potential structure cooperating with waves, *Ann. Geophys.*, *18*, 596.

Mozer, F. S., and A. Hull (2001), The origin and geometry of upward parallel electric fields in the auroral acceleration region, *J. Geophys. Res.*, *106*, 5763.

Rönnmark, K. (1999), Electron acceleration in the auroral current circuit, *Geophys. Res. Lett.*, *26*, 983.

Southwood, D. J., and W. J. Hughes (1983), Theory of hydromagnetic waves in the magnetosphere, *Space Sci. Rev.*, *35*, 301.

Stern, D. P. (1981), One-dimensional models of quasi-neutral parallel electric fields, *J. Geophys. Res.*, *86*, 5839.

Wright, A. N. (1996), Transfer of magnetosheath momentum and energy to the ionosphere along open field lines, *J. Geophys. Res.*, *101*, 13,169.

Wright, A. N., W. Allan, M. R. Ruderman, and R. C. Elphic (2002), The dynamics of current carriers in standing Alfvén waves: Parallel electric fields in the auroral acceleration region, *J. Geophys. Res.*, *107*(A7), 1120, doi:10.1029/2001JA900168.

Wright, A. N., W. Allan, and P. A. Damiano (2003), Alfvén wave dissipation via electron energization, *Geophys. Res. Lett.*, *30*(16), 1847, doi:10.1029/2003GL017605.

A. N. Wright, Mathematical Institute, University of St. Andrews, St. Andrews, Fife KY16 9SS, UK. (andy@mcs.st-and.ac.uk)